Making **Ea**rth **S**cience Data Records for **U**se in **R**esearch **E**nvironment**s** (MEaSUREs)

README Document for the TOMSN7AER, TOMSEPAER and OMIAuraAER Aerosol Products

Goddard Earth Sciences Data and Information Services Center (GES DISC)

NASA Goddard Space Flight Center, Greenbelt, MD 20771 USA

Principal Investigators: Omar Torres, Pawan K. Bhartia, GSFC Code 614
omar.o.torres@nasa.gov
301-614-6776

Algorithm Developer: Changwoo Ahn, SSAI, GSFC Code 614
changwoo.ahn@ssaihq.com
301-867-2171

Algorithm Support: Peter J.T. Leonard, ADNET, GSFC Code 619
peter.j.leonard@nasa.gov
301-352-4659

Revision History

Revision Date	***Changes***	***Authors***
3 October 2018	First Release	Omar Torres & Peter Leonard
1 November 2018	Corrected Equation 1 to be consistent with the explanation. Corrected the table numbers in Section 2.3.2 and 2.3.6	Peter Leonard & Jian Zeng

TABLE OF CONTENTS

1. INTRODUCTION

1.1 MEaSUREs Near UV Aerosol Products

This document describes a multi-decadal Fundamental Climate Data Record (FCDR) of calibrated radiances as well as an Earth System Data Record (ESDR) of aerosol properties over the continents derived from a 32-year record of satellite near-UV observations by three sensors. Table 1 lists the instruments, record length, observation channels, and associated MEaSUREs aerosol product.

Instrument/Agency	Resolution	Operation Period	Aerosol Channels (λ, λ_0)	MEaSUREs Product (ESDR ShortName)
N7-TOMS/NASA	50 km	Oct. 1978 - May 1993	339.7, 379.9	TOMSN7AER
EP-TOMS/NASA	40 km	Jun. 1996 - Dec. 2005	331.2, 360.4	TOMSEPAER
Aura-OMI/KNMI	13x24 km	Aug. 2004 - Present	354.0, 388.0	OMIAuraAER

Table 1. The near UV sensors and MEaSUREs products.

Radiance observations at the wavelengths listed in Table 1 made by the Total Ozone Mapping Spectrometer (TOMS) sensors on the Nimbus 7 (N7) and Earth Probe (EP) satellites, along with the Ozone Monitoring Instrument (OMI) on the EOS-Aura spacecraft were used in this MEaSUREs NASA-funded project. Calibrated near UV radiances were used in conjunction with accurate radiative transfer calculations in a retrieval algorithm to derive the UV Aerosol Index (UVAI) as well as quantitative aerosol parameters such as aerosol extinction optical depth (AOD) and aerosol single scattering albedo (SSA) from which absorption optical depth (AAOD) can be calculated. Daily UVAI values were derived over both the oceans and the continents. Although the aerosol optical depth retrieval was intended mainly over land, the retrieval algorithm was also applied over the oceans to ensure spatial continuity across coastal areas. Documented FCDR's and ESDR's are global calibrated radiances, daily UVAI, and daily and monthly mean values of aerosol AOD, SSA and AAOD. Although a common retrieval algorithm was applied to radiance observations by the sensors in Table 1, some algorithmic differences remain as discussed in Section 2 of this document.

1.2 Satellite Instruments

1.2.1 Nimbus 7 TOMS

The first TOMS sensor was launched on October 24 1978 onboard the Nimbus 7 (N7) satellite into a sun synchronous orbit with an inclination angle of 99.1 degrees and altitude 960 km. The N7-TOMS sensor was part of a multi-instrument payload that included eight additional sensors. The observation record goes from 1978 October 31 to 1993 May 6. TOMS is a fixed-grating Ebert-Fastie mono-chromator with photomultiplier tube detector that measures solar backscattered ultraviolet (BUV) radiances (I) at six narrow wavelengths bands in the near ultraviolet (UV) spectral region as well as the incident solar irradiances (F) (Heath, *et al*., 1975). The ratio of radiance to irradiance provides the spectral reflectivity parameter used in the retrieval of atmospheric constituents. Table 1 shows the pairs of non-absorbed wavelengths used to account for surface and cloud reflectivity (R) and its spectral dependence. These non-absorbed wavelengths are used to retrieve information on aerosol properties.

N7-TOMS scanned in the cross-track direction in 3^o steps from 51^o on west side of nadir to 51^o on the east, for a total of 35 cross-track samples. The instantaneous field-of-view (FOV) of 3^o x 3^o results in a footprint varying from a 50 km x 50 km square FOV at nadir to a 125 km by 280 km diamond-shaped FOV at the scan extremes. The total swath width is 3000 km covering the entire Earth’s surface in 14 orbits per day.

1.2.2 Earth Probe TOMS

EP-TOMS was launched on a dedicated satellite on July 2, 1996. The experiment used a single monochromator and scanning mirror to sample the backscattered solar ultraviolet radiation at 35 sample points at 3° intervals along a line perpendicular to the orbital plane. Regular measurements began on July 25 from the initially planned orbit of 500 km at an inclination of 98° and a local equator crossing time of 11:16. The EP-TOMS experiment reported measurements of backscattered Earth radiance in the six 1-nm bands. Following the failure of the ADEOS-1 mission carrying a previously deployed TOMS instrument, in December of 1997, the EP-TOMS orbit was elevated to an altitude of 739 km with an inclination of 98.4°. The local equator crossing time was unchanged. The higher orbit resulted in 90% daily global coverage (84% at equator and 100% at 30° latitude) with a 40-km nadir spatial resolution. The wavelength pair listed in Table 1 is used for the aerosol properties retrieval.

1.2.3 Aura OMI

The Ozone Monitoring Instrument (OMI) is a high-resolution spectrograph that measures the upwelling radiance at the top of the atmosphere in the ultraviolet and visible (270–500 nm) regions of the solar spectrum [*Levelt et al.,* 2006]. It is one of four sensors on the EOS-Aura platform. It has a 2600-km wide swath and provides daily global coverage at a spatial resolution varying from 13 km x 24 km at nadir to 28 km x 150 km at the extremes of the swath. Aura is in a sun-synchronous orbit with ascending node local equator crossing time of 13:45. The Aura spacecraft is part of the A-train, which includes three other aerosol sensors Aqua-MODIS, Parasol, and CALIPSO. The OMI project is a joint effort by the Netherlands, Finland, and the USA. The wavelength pair listed in Table 1 is used for the aerosol properties retrieval.

1.3 Science Background

The detection capability of aerosols from space-borne observations in the UV was developed nearly two decades ago at the NASA Goddard Space Flight Center [*Torres and Remer,* 2013] as the fortunate, unintended result of an upgrade of the TOMS ozone retrieval algorithm. The TOMS algorithm rests on the assumption that in an atmospheric column the UV scattering effects of tropospheric aerosols and clouds, as well as surface reflection, can be represented by a hypothetical wavelength independent Lambertian reflector at the bottom of the atmospheric column. The Lambert Equivalent Reflectivity (LER) of this “effective surface” is determined from radiance measurements at λ_0, a channel insensitive to ozone absorption, using radiative transfer calculations for a molecular-only atmosphere.

In the upgrade to the TOMS Version 7 ozone retrieval algorithm, a spectral residual quantity, intended to test the validity of the LER spectral neutrality assumption was introduced. Such residual quantity was simply the resulting LER difference at the λ_0 and λ channels after correcting for small ozone absorption effects. When mapping the global spatial distribution of this residual quantity it became apparent that although the lack of wavelength dependence assumption held in most cases yielding a nearly zero LER difference, in the presence of desert dust and carbonaceous aerosol layers the assumption broke down resulting in LER differences as large of 3 [*Hsu et al.,* 1996]. The residual quantity was later modified to its current form (see Equation 3) in terms of radiances [*Herman et al.,* 1997; *Torres et al.,* 1998]. The observed aerosol absorption signal turned out to come from the interaction of particle absorption and molecular scattering [*Torres et al.,* 1998] generating a spectral signal that deviates from that of Rayleigh scattering. Because most of the occurrences of non-zero values of this residual quantity are associated with particle UV absorption the term UV Aerosol Index (UVAI) was coined.

The UVAI detects absorbing aerosols over ocean and land surfaces including deserts and for both cloud-free and partly cloudy skies [*Hsu et al*., 1996; *Herman et al.,* 1997; *Torres et al,* 1998]. It also

detects aerosols above clouds [*Torres et al., 2012*; *DeGraaf et al*, 2010], and above extremely bright backgrounds such as ice and snow-covered surfaces [*Hsu et al.*, 1999; *Torres et al.*, 2007]. These properties make the UVAI an excellent global tracer of carbonaceous aerosols and desert dust, which are, by far, the most predominant components of the atmospheric aerosol load.

The next step in the utilization of near UV observations for aerosol sensing was the quantitative interpretation of the UVAI information content in terms of physically meaningful parameters. Satellite measured radiances at two near-UV channels in the range 330-390 nm are used as input to the algorithm that derives simultaneously aerosol optical depth and single scattering albedo under cloud-free conditions [*Torres et al*, 1998; 2007; 2013]. The inversion procedure uses tabulated radiative transfer calculations for a number of assumed aerosol models. A description of the AERUV algorithm follows in Section 2.

2. MULTI-SATELLITE AEROSOL ALGORITHM

This section provides a brief description of the near UV aerosol retrieval algorithm applied to observations by the N7 and EP TOMS sensors, as well as the Aura-OMI instrument. For each sensor, the algorithm uses observations at the aerosol channels λ *and* λ_0 in Table 1.

2.1 Ancillary Information

2.1.1 Surface Albedo

Global climatological data sets of Lambertian surface reflectivity (R_{SFC}) at 331, 340, 360, and 380 nm are used to account for surface effects in the algorithms applied to the two TOMS sensors. It was obtained using a multi-year record of scene reflectivity (R_{SCE}) obtained from N7-TOMS observations. A similar analysis was carried out based on OMI long-term record to derive R_{SFC} at 354 and 388 nm. For a Lambertian reflecting surface the satellite measured radiance at the top of the atmosphere can be estimated using the Chandresekar approximation (Equation 1),

$$I^{obs} = I^{0} + \frac{RT}{1 - S\,R} \qquad (1)$$

where I^{obs} represents the satellite measured radiance and, I^{0}, T, and S are respectively the modeled path radiance, the two-way transmittance, and the spherical albedo of a molecular atmosphere, and R is simply the Lambertian reflectivity of the of bottom of the atmospheric column that in addition to the actual surface, also includes clouds and aerosol effects. Scene Lambert Equivalent Reflectivity (LER) values at 331, 340, 360, and 380 nm (R_{SCE}) are calculated at every Nimbus 7 TOMS pixel for a purely molecular atmosphere model solving for the R term in Equation 1 yielding

$$R_{SCE} = \frac{I^{obs} - I^{0}}{T + S\left(I^{obs} - I^{0}\right)} \qquad (2)$$

Multi-year long R_{SCE} records from N7-TOMS (1979-1992) and OMI (2005-2015) observations have been used to create monthly climatologies of surface reflectivity (R_{SFC}) using the approach described below.

Over land, monthly R_{SFC} values are estimated as the minimum observed R_{SCE} over the multi-year TOMS and OMI records. Resulting values for every month of the year averaged over a 0.5°x0.5° geographical grid.

The ocean surface reflectivity is estimated in a similar way as over land with the addition of a correction for the Sun's specular reflection. The satellite derived R_{SCE} under cloud-free conditions over the ocean is approximated as the sum of two terms: a Lambert-equivalent Fresnel reflectivity (R_F) term and a second reflectivity term associated with water-leaving reflectance (R_W). The R_F term is obtained by calculating the upwelling radiance at the top of the atmosphere using an atmosphere-ocean radiative transfer model [*Cox and Munk*, 1954] for a chlorophyll-free ocean. The calculated radiance is then converted to LER using an equation similar to Eq. 1, in which the calculated radiance is used in lieu of the observed one. The R_F thus calculated varies with solar zenith, view zenith and azimuth angles. R_W is estimated empirically by subtracting R_F from R_{SCE}. The resulting minimum R_W values per grid per month are assumed here to represent the ocean $R_{SFC.}$

2.1.2 Aerosol Layer Height

The height above the surface of absorbing aerosol layers (desert dust and smoke particles) is given by a climatological data set derived from CALIOP observations [*Torres et al.,* 2013]. Although the climatology covers most regions of the globe where seasonally varying atmospheric loads of desert dust and carbonaceous aerosols are known to reside, there are cases where the CALIOP data base does not provide height information. In those instances, the height of desert dust (DST) aerosol layers is taken from a GOCART-generated climatology [*Ginoux et al.,* 2001]. A detailed description of aerosol layer height determination is given in Section 3.2.2.

Because of the absence of global information on aerosol layer height during the period of operation of the TOMS sensors, the CALIOP climatology is retroactively applied to the TOMS aerosol algorithms. In doing this, it is assumed that the resulting data set on aerosol layer height derived from active satellite observations in the 2006-2008 period, is climatologically equivalent to the prevailing conditions in the 1979-2001 period of operation of the TOMS instruments.

2.1.3 AIRS Carbon Monoxide (CO) Data

Since CO is the main gaseous component of biomass burning emissions, it constitutes a reliable tracer of carbonaceous aerosol plumes. Total column CO measurements in molecules-cm^{-2} have been reported by the Atmospheric Infrared Sounder (AIRS) on the Eos-Aqua satellite. As used in TOMS and OMI aerosol algorithms, the Version 6 AIRS3STD CO total column in molecules-cm^{-2} is reduced to a unit-less index (COI), by dividing the AIRS reported CO measurement by 10^{18} molecules-cm^{-2}. A monthly COI climatology based on multi-year (2003-2015) CO observations has been produced to aid in the identification of carbonaceous aerosols [*Torres et al.,* 2013]. As with the CALIOP aerosol layer height, the CO climatology is used retroactively as a proxy of the prevailing monthly average CO spatial distribution during the time of 1979-2001 period of operation of the TOMS sensors. Real-time as well as climatological COI values are used in the OMI aerosol algorithm as discussed is Section 2.2.

2.2 Aerosol Retrievals

2.2.1 UV Aerosol Index and Cloud Fraction

UVAI is a measure of the departure of the *observed* spectral dependence of the near-UV upwelling radiation at the top of the actual Earth surface-atmosphere system from that *calculated* for a hypothetical pure molecular atmosphere bounded at the bottom by a wavelength independent Lambertian

surface. UVAI is calculated as shown in Eq. 3, where λ and λ_0 are the wavelengths listed in Table 1 for each sensor. λ_0 is the reference wavelength whereas λ is the wavelength at which UVAI is calculated.

$$UVAI = -100\left\{\log\left[\frac{I_{\lambda}^{obs}}{I_{\lambda_0}^{obs}}\right] - \log\left[\frac{I_{\lambda}^{cal}}{I_{\lambda_0}^{cal}}\right]\right\} = -100\log\left[\frac{I_{\lambda}^{obs}}{I_{\lambda}^{cal}}\right] \qquad (3)$$

The calculated radiances are obtained by assuming that the radiance measured by the sensor at pixel level emanates from a combination of clear and cloudy conditions (I_{λ}^{s} and I_{λ}^{C}) involving a cloud of fixed optical depth and varying cloud fraction. The I_{λ}^{s} term is calculated from the Chandresekar equation using as input the wavelength dependent climatological values of surface albedo (derived as explained in Section 2.1.1) and a pure molecular atmospheric model for surface pressured adjusted for topography. The I_{λ}^{C} terms, on the other hand, are calculated using Mie scattering theory for an assumed water cloud model [*Deirmendjian*, 1964] and wavelength-dependent refractive index [*Hale and Querry*, 1973], at prescribed top and bottom levels (700 and 800 hPa), and fixed cloud optical depth (COD) of 10. The choice of COD value of 10 is based on the highest frequency of occurrence of this value reported by MODIS observations [*King et al.*, 2013]. A wavelength independent radiative cloud fraction, f_C, is calculated from equation

$$f_C = \frac{I_{\lambda_0}^{obs} - I_{\lambda_0}^{s}}{I_{\lambda_0}^{C} - I_{\lambda_0}^{s}} \qquad (4)$$

When the resulting cloud fraction is larger than unity, overcast sky conditions are assumed (i.e., $f_C=1.0$), and a new I_{λ}^{C} term for COD value larger than 10 that matches $I_{\lambda_0}^{obs}$ is derived. I_{λ}^{cal} values are then obtained by linearly combining the clear and cloudy sky contributions:

$$I_{\lambda}^{cal} = (1.0 - f_C) I_{\lambda}^{s} + f_C I_{\lambda}^{C} \qquad (5)$$

For snow/ice conditions at the surface, a Lambertian reflectivity term is calculated as

$$R_{\lambda_0} = \frac{I_{\lambda_0}^{obs} - I_{\lambda_0}^{0}}{T_{\lambda_0} + S_{\lambda_0}(I_{\lambda_0}^{obs} - I_{\lambda_0}^{0})} \qquad (6)$$

The terms in Eq. 6 have been defined in Section 2.1. The calculated radiance is then obtained from the expression

$$I_{\lambda}^{cal} = I_{\lambda}^{0} + \frac{R_{\lambda_0} T_{\lambda}}{1 - S_{\lambda} R_{\lambda_0}} \qquad (7)$$

where a wavelength-independent Lambertian reflectivity has been assumed. The output of this calculation is then fed into Eq. 3 to calculate UVAI. If a snow or ice fraction is available, UVAI is calculated as a weighted combination of the resulting UVAI's using Equations 5 and 7 for obtaining the calculated component.

Near-zero values of UVAI result when the radiative transfer processes accounted for in the simple Rayleigh scattering model adequately explain the observations. For a well-calibrated sensor, the non-zero UVAI values are produced solely by geophysical effects, of which absorbing aerosols are by far the most important. Non-absorbing aerosols yield small negative UVAI values but the

difficulty to separate the non-absorbing aerosol signal from other non-aerosol related effects limits its usefulness.

2.2.2 Aerosol Optical Depth and Single Scattering Albedo

In addition to the qualitative UVAI and cloud fraction parameters, the algorithm derives the aerosol optical depth (AOD) and the imaginary component of the refractive index at 388 nm. The single scattering albedo (SSA) associated with the assumed aerosol particle size distribution (PSD) and the retrieved 388 nm imaginary component of the refractive index is calculated. A set of AOD/SSA parameters is reported for pixels deemed to be free of cloud contamination. Because the current characterization of ocean reflective properties in the algorithm does not explicitly account for ocean color effects, the quality of the retrieved aerosol properties over the oceans for low aerosol amounts would be highly uncertain. For that reason, retrievals over the oceans are only carried out for high concentrations of either desert dust or carbonaceous aerosols when the *AI* values are larger than or equal to 1.0 over the oceans, *AI* values less than 1.0 are assumed to be associated with ocean color effects and/or low concentration weakly absorbing (or non-absorbing) aerosols.

2.3 Algorithm Description

2.3.1 Aerosol Models

The retrieval algorithm assumes that one of three types of aerosols can represent the column atmospheric aerosol load: desert dust (DST), carbonaceous aerosols associated with biomass burning (CRB), and sulfate-based urban-industrial aerosols (SLF). For the three aerosol types, the PSD is given by a bi-modal distribution function whose parameters are listed in Table 2. Each aerosol type is represented by seven aerosol models of varying single scattering albedo, for a total of twenty-one models. The CRB and SLF aerosol types are modeled as polydispersions of spherical particles. The DST aerosol type is modeled as spheroids [*Torres et al.*, 2017; *Gassó and Torres*, 2016]. Radiance look-up tables at λ and λ_0 with nodal points on viewing geometry, AOD, SSA and aerosol layer height are created using Mie Theory for spherical particles and T-matrix and Geometric Optics for spheroids [*Dubovik et al.*, 2006].

Aerosol Type	**DST**	**CRB**	**SLF**
Fine mode radius, r_f (μm)	0.0520	0.0803	0.0880
Fine mode standard deviation, σ_f (μm)	1.697	1.492	1.499
Minimum r_f (μm)	0.0063	0.0162	0.0174
Maximum r_f (μm)	0.4312	0.3971	0.4445
Coarse mode radius, r_c (μm)	0.6700	0.7055	0.5093
Coarse mode standard deviation, σ_c(μm)	1.806	2.075	2.160
Minimum r_c (μm)	0.0630	0.0381	0.0234
Maximum rc (μm)	7.1276	13.0788	11.0858
Fine mode particle concentration #/cm^2	13.531	13.2371	6.523
Coarse mode particle concentration #/cm^2	0.0588	0.0023	0.0026
Real Refractive Index (n)	1.55	1.50	1.40
Imaginary refractive index ratio ($k_\lambda/k_{\lambda 0}$)	1.40	1.2	1.20

Table 2. Particle size distribution parameters and optical properties of assumed aerosol types.

Aerosol PSD parameters listed in Table 2 are based on published ground-based AERONET observations. Also listed in Table 2 are the assumed wavelength –independent real component of the refractive index, and the ratio of imaginary component of refractive index, *k*, between the wavelength-pairs ($k_\lambda/k_{\lambda 0}$) in Table 1.

2.3.2 Aerosol type selection

Aerosol type determination is carried out based on the magnitudes of the UVAI and COI parameters as illustrated in Fig. 1. Because of the lack of AIRS daily coverage, it is not always possible to use same-day COI values to infer aerosol type. Depending on AIRS data availability, COI may be determined based on current-day observations, previous day observations, or a monthly climatology. The actual source of COI data is documented in the AIRS_CO_Flags dataset with values from 1 to 3 as shown in Table 3.

Value of *AIRSCO_Flags* data field	**Source of COI data**
1	Current day
2	Previous day
3	Monthly Climatology

Table 3. The CO Index determination.

Threshold values of UVAI ($UVAI_0$) are 0.8 over land, and 1.0 over the oceans. COI threshold values (COI_0) are 2.0 and 1.6 for the northern and southern hemisphere respectively. COI threshold values are intended to remove background upper tropospheric CO which may not be necessarily associated with carbonaceous aerosols. A smoothing function in COI_0 is used to transition from SH to NH threshold values.

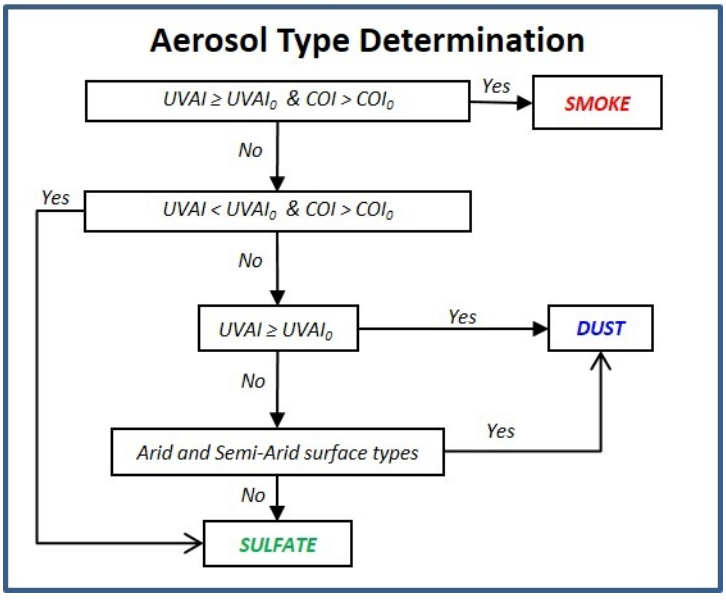

Figure 1. A flow diagram illustrating the aerosol type selection scheme.

2.3.3 Cloud Screening

Because of the coarse sensors resolution sub-pixel cloud contamination is the largest source of uncertainty in retrieved quantitative TOMS and OMI aerosol products. In the algorithm the level of cloud contamination is determined in a decision tree using a combination of thresholds in reflectivity, R_{SFC} and ΔR (R_{SCE} - R_{SFC}), COI and UVAI as shown in Fig. 2.

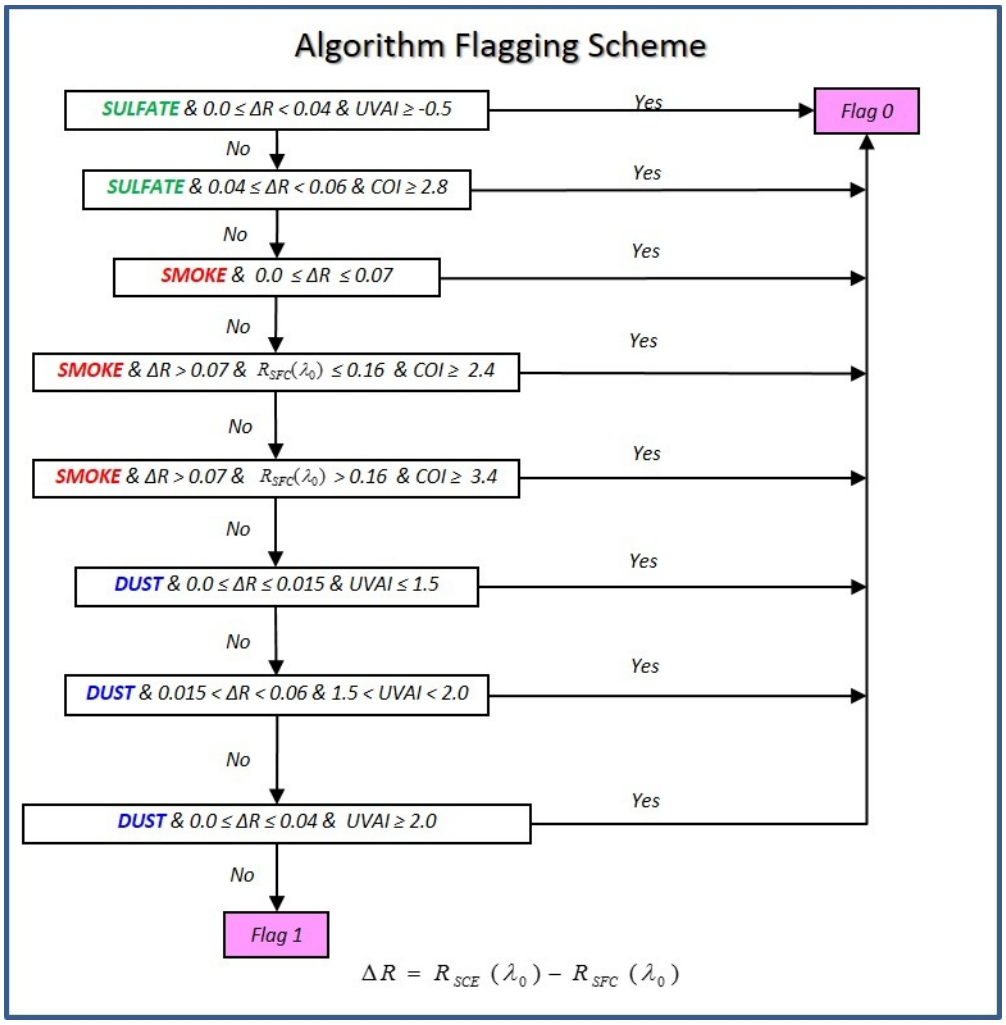

Figure 2. The criteria for identifying cloud-free pixels.

Algorithm quality Flags 0 and 1 assign a level of confidence to the retrieved parameters. Flag 0 (highest confidence) is assigned to retrieval conditions when minimum cloud contamination was detected, whereas Flag 1 is reported for conditions where cloud contamination is suspected. Although, the data is still reported for Flag 1 retrievals, its quantitative use is not recommended. Because cloud contamination affects AOD and single scattering co-albedo (1-SSA) in opposite directions, a partial cancellation of errors may take place in the calculation of AAOD.

2.3.4 Aerosol layer height

The assumed aerosol level height is extracted from the CALIOP height climatology for each pixel. Although the CALIOP climatology provides information on aerosol layer height for most of the globe, there may be instances when no data is available. In those cases, the choice of aerosol layer height for absorbing aerosol layers varies with aerosol type and location.

Carbonaceous aerosol layers within 30 degrees of the Equator are assumed to have maximum concentration at 3 km above ground level; whereas smoke layers at mid and high-latitude (poleward of ±45˚) are assumed to peak at 6 km. The height of smoke layers between 30˚ and 45˚ latitude in both hemispheres is interpolated between 3 and 6 km with latitude.

The height of desert dust aerosol layers varies between 1.5 and 10 km, and is taken from a multi-year climatological average of Chemical Model Transport (CTM) calculations using the GOCART model.

Value of *HeightFlags* data field	Source of aerosol layer height information
1	CALIOP Climatology
2	GOCART Climatology
3	Interpolated with latitude between 3 and 6 km
4	Assumed value (0.0, 1.5, 3.0, 6.0, or 10.0)

Table 4. The aerosol layer height determination.

For the sulfate-based aerosols, the algorithm considers that the aerosol concentration is largest at the surface and decreases exponentially with height. The *HeightFlags* dataset provides information on the source of aerosol layer height used in the AOD/SSA retrieval. Value of *HeightFlags* varies from 1 to 4 as shown in Table 4.

2.3.5 Inversion Scheme

Surface Category	*AI*	COI	Surface Type	Aerosol Type	Retrieved Parameters
Ocean	≥ 1.0	>2.0 NH (1.6 SH)	n/a	Smoke	AOD, SSA
Ocean	≥ 1.0	≤2.0 NH (1.6 SH)	n/a	Dust	AOD,SSA
Ocean	<1.0	-	-	-	No retrieval
Land	≥ 0.8	>2.0 NH (1.6 SH)	All	Smoke	AOD,SSA
Land	≥ 0.8	≤ 2.0 NH (1.6 SH)	All	Dust	AOD,SSA
Land	< 0.8	>2.0 NH (1.6 SH)	All	Sulfate	AOD,SSA
Land	< 0.8	≤ 2.0 NH (1.6 SH)	All but arid	Sulfate	AOD,SSA
Land	< 0.8	≤ 2.0 NH (1.6 SH)	arid	Dust	AOD,SSA

Table 5. The retrieval approach criteria.

A summary of the retrieval criteria and retrieved parameters is presented in Table 5. As stated, retrievals take place over land for all cloud-free conditions. In addition of cloud-free conditions, the AI must be greater than unity for ocean retrievals.

Retrieved values of AOD, AAOD and SSA are reported at λ_0. Similar values are also reported at λ (see Table 1) and at 500 nm by conversion from the retrieval at λ_0. The wavelength conversion from λ_0 to λ and 500 nm is done using the spectral dependence associated with the assumed aerosol particle size distribution and retrieved absorption information.

2.3.6 Algorithm Flag

A simplified algorithm flag scheme has been implemented. Flag categories and their description are summarized in Table 6. Flags 0 and 1 qualify the reliability of reported retrieved parameters in terms of sub-pixel cloud contamination effects. Flag 1 is reported for conditions where cloud contamination was suspected to be present. Although, the data is still reported for Flag 1 retrievals, its quantitative use is not recommended. Flags 3 through 7 indicate the occurrence of observational, geographical or environmental conditions preventing the retrieval of aerosol parameters and fill values for the retrieved parameters are reported in the respective pixel. Flag 8 is used to identify pixels affected by a condition

known as the cross track or “row” anomaly. It consists on an external blockage affecting the quality of the Level 1B radiance data at all wavelengths for a number of OMI viewing directions. The affected viewing positions correspond to rows on the CCD detectors, and hence the term “row anomaly” is used to refer to this instrumental issue. The OMI row anomaly changes over time, and affects the quality of OMI Level 2 data products. By means of radiances analysis, row anomalies are identified and flagged by KNMI in the XTrackQualityFlags field of the OMI L1B data.

Flag	Description
0	Minimum sub-pixel cloud contamination. Most reliable retrievals(AOD, SSA, AAOD)
1	Possible Cloud contaminated retrievals, retrievals still reported.
2	No longer used.
3	Out-of-bounds SSA or AOD above 6.0 at 500nm.
4	Snow/ice contaminated data.
5	Solar Zenith Angle above threshold (70 degree).
6	Sun glint angle below threshold over water (40 degree).
7	Terrain Pressure below threshold (250.0 hPa).
8	Cross track anomaly.

Table 6. The algorithm flag scheme.

Starting with algorithm version 1.4.2, a row anomaly flagging scheme developed for the NASA OMI Total Ozone (OMTO3) product has been adopted in OMIAuraAER. In the OMTO3-based approach anomaly affected rows are identified determined through analysis of averages for each row of previous ten days of data. Upon reprocessing, the flags for each ten day period are determined using data from the same period. In OMIAuraAER row anomaly affected pixels are assigned Algorithm Flag 8 as shown in Table 2 and fill values are reported in the respective pixel.

3. DATASET ORGANIZATION

The TOMSN7AER, TOMSEPAER and OMIAuraAER products are Level 2 swath data files that follow a specific file naming convention and dataset organization.

3.1 File Naming Convention

The product files are named as in this example:

TOMS-N7_L2-TOMSN7AER_1991m0630t084305-o64302_v02-00-2017m1018t090804.h5

The components of file names are as follows:

1. Instrument (TOMS)
2. Spacecraft (N7)
3. Process Level (L2)
4. ESDT Short Name (TOMSN7AER)
5. Date and Time at Start of Orbit (1991-06-30 08:43:05 UTC)
6. Orbit Number (64302)
7. Product Version (02-00)
8. Production Date and Time (2017-10-18 09:08:04 UTC)
9. File Type (h5)

3.2 File Format and Structure

The product files are in plain HDF5 that is netCDF4-compatible and CF-compliant. Each product file contains global attributes, dimensions, an ancillary data group, a geolocation data group, a science data group, and a sensor data group.

3.3 Key Science Datasets

There are several key science datasets in the science data group in each product file. The first releases of the TOMSN7AER and TOMSEPAER products only contain the key datasets described below for UV aerosol index and cloud fraction.

3.3.1 FinalAerosolAbsorptionOpticalDepth

Each FinalAerosolAbsoprtionOpticalDepth dataset contains the best solution aerosol absorption optical depth for the wavelength provided in the dataset name. The values at 500 nm are extrapolated.

3.3.2 FinalAerosolOpticalDepth

Each FinalAerosolOpticalDepth dataset contains the best solution aerosol optical depth for the wavelength provided in the dataset name. The values at 500 nm are extrapolated.

3.3.3 FinalAerosolSingleScatteringAlbedo

Each FinalAerosolSingleScatteringAlbedo dataset contains the best solution aerosol single scattering albedo for the wavelength provided in the dataset name. The values at 500 nm are extrapolated.

3.3.4 FinalAerosolLayerHeight

The FinalAerosolLayerHeight dataset contains the best solution for the aerosol layer height for the pair of wavelengths provided in the dataset name.

3.3.5 FinalAlgorithmFlags

The FinalAlgorithmFlags dataset contains the best solution for the algorithm flag for the pair of wavelengths provided in the dataset name.

3.3.6 UVAerosolIndex and CloudFraction

Each UVAerosolIndex dataset contains the calculated aerosol index for the pair of wavelengths provided in the dataset name, and the CloudFraction dataset contains the corresponding calculated cloud fraction.

4. DATA CONTENTS

Each TOMSN7AER, TOMSEPAER and OMIAuraAER product file contains global attributes, dimensions, an ancillary data group, a geolocation data group, a science data group, and a sensor data group. This section provides specific details regarding these components.

4.1 Global Attributes

There are 43 file-level (global) attributes in each product file as shown in Figure 3.

Name	Value
AuthorAffiliation	NASA/GSFC
AuthorName	O. Torres, et al.
Conventions	CF-1.6
DataSetQuality	Under investigation.
DayNightFlag	Day
EastBoundingCoordinate	180.0
EquatorCrossingDate	2006-08-15
EquatorCrossingLongitude	-0.78
EquatorCrossingTime	13:47:00
FOVResolution	13x24km
GranuleDay	15
GranuleDayOfYear	227
GranuleMonth	8
GranuleYear	2006
HDFVersion	5-1.8.12
InputPointer	OMI-Aura_L1-OML1BRVG_2006m0...
InstrumentShortName	OMI
LocalGranuleID	OMI-Aura_L2-OMIAuraAER_2006...
LocalityValue	Global
LongName	OMI/Aura Near UV Aerosol Index,...
NorthBoundingCoordinate	89.8501
NumTimes	1643
OrbitNumber	11086
PGEVersion	0.0.6
ParameterName	Near UV Aerosol Properties
PlatformShortName	Aura
ProcessLevel	2
ProcessingCenter	ACPS
ProductType	L2 Swath
ProductionDateTime	2018-02-08T11:23:32.0Z
RangeBeginningDate	2006-08-15
RangeBeginningTime	13:02:41
RangeEndingDate	2006-08-15
RangeEndingTime	14:41:33
SensorShortName	CCD Ultra Violet
ShortName	OMIAuraAER
Source	Aura/OMI
SouthBoundingCoordinate	-81.36225
TAI93At0zOfGranule	4.29753606E8
VersionID	3
WestBoundingCoordinate	-180.0
identifier_product_doi	10.5067/MEASURES/AER/DATA203
identifier_product_doi_authority	http://dx.doi.org/

Figure 3. The file-level (global) attributes of the OMIAuraAER product.

4.2 Dimensions

There are six dimensions in each product file as show in Figure 4:

nCorners - The dimension representing the four ground-pixel corners.
nLevels - The dimension representing the atmospheric level.
nTimes - The dimension representing the scan-line number.
nWavel2 - The dimension representing the wavelengths for reflectivity.
nWavel3 - The dimension representing the wavelengths for surface albedo and normalized radiance.
nXtrack - The dimension representing the cross-track positions.

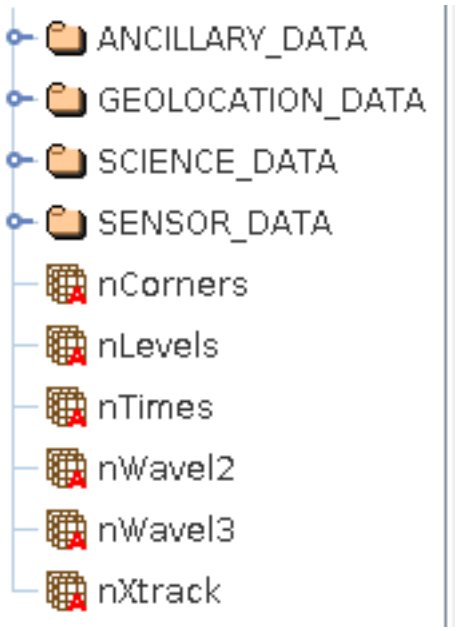

Figure 4. The four groups and six dimensions in the OMIAuraAER product.

4.3 Datasets

4.3.1 Ancillary Data

There are four datasets in the ancillary data group in each product file. These data are from external sources, and are required to carry out the retrievals.

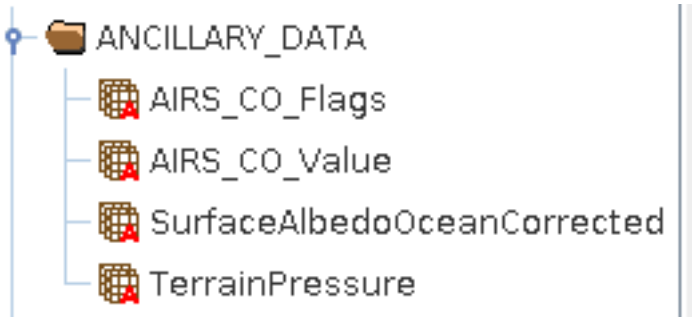

Figure 5. The ancillary data group the OMIAuraAER product.

4.3.2 Geolocation Data

There are several datasets in the geolocation data group in each product file as shown in Figure 6. This includes longitude and latitude for the ground-pixel centers and the ground-pixel corners.

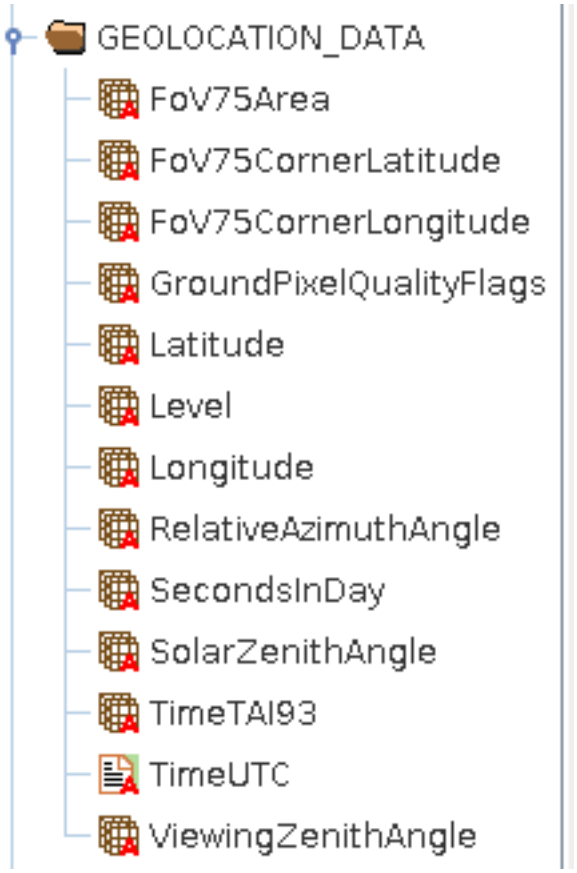

Figure 6. The geolocation data group of the OMIAuraAER product.

4.3.3 Science Data

There are many datasets in the science data group in each product file as shown in Figure 7. This includes the final aerosol absorption optical depth, final aerosol optical depth and final aerosol single scattering albedo at various wavelengths, and UV aerosol index. The first releases of the TOMSN7AER and TOMSEPAER products only contain cloud data, normalized radiance, reflectivity, residue and UV aerosol index in the science data group.

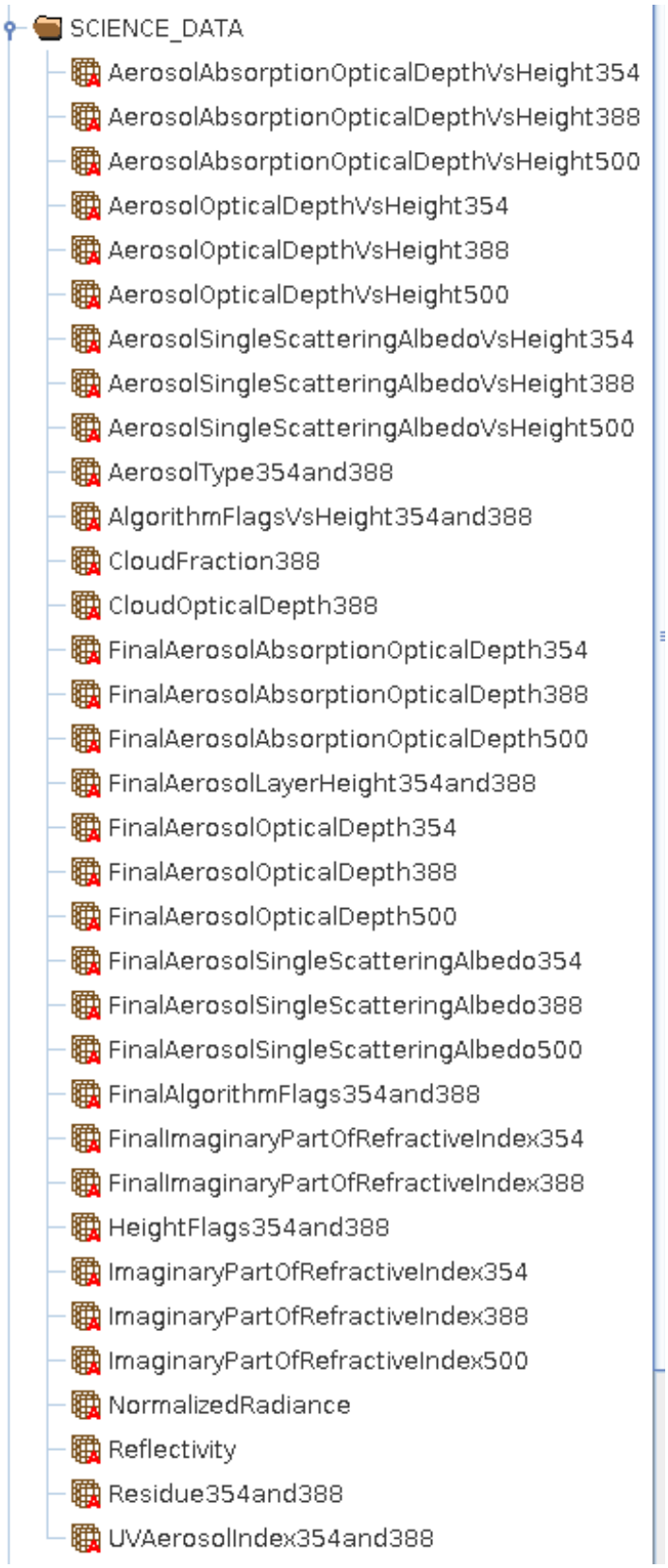

Figure 7. The science data group of the OMIAuraAER product.

4.3.4 Sensor Data

There is one dataset in the sensor data group in each product file as show in Figure 8, which contains the wavelengths used.

Figure 8. The sensor data group of the OMIAuraAER product.

5. CONTACTS

Principal Investigators: Omar Torres, Pawan K. Bhartia, GSFC Code 614
omar.o.torres@nasa.gov
301-614-6776

Algorithm Developer: Changwoo Ahn, SSAI, GSFC Code 614
changwoo.ahn@ssaihq.com
301-867-2171

Algorithm Support: Peter J.T. Leonard, ADNET, GSFC Code 619
peter.j.leonard@nasa.gov
301-352-4659

6. REFERENCES

Cox, C., and W. Munk (1954) Measurement of the roughness of the sea surface from photographs of the Sun's glitter, J. Opt. Soc. Amer., 44, 838–850

Dave, J.V., and C. L. Mateer, A preliminary study on the possibility of estimating total atmospheric ozone from satellite measurements, *J. Atm. Sci*., 24, 414–427, 1967

Deirmendjian, D. (1964), Scattering and polarization properties of water clouds and hazes in the visible and infrared, Appl. Opt., 3, 187–196

Dubovik, O., et al. (2006), Application of spheroid models to account for aerosol particle nonsphericity in remote sensing of desert dust, J. Geophys. Res., 111, D11208, doi:10.1029/2005JD006619

Gassó, S. and Torres, O.: The role of cloud contamination, aerosol layer height and aerosol model in the assessment of the OMI near-UV retrievals over the ocean, Atmos. Meas. Tech., 9, 3031-3052, doi:10.5194/amt-9-3031-2016, 201

Ginoux, P., M. Chin, I. Tegen, J. Prospero, B. Holben, D. Dubovik,and S. J. Lin, 2001: Sources and distributions of dust aerosols simulated with the GOCART model. *J. Geophys. Res.*, 106, 20,255–20,273.

Hale, G. and M. Querry, (1973), Optical Constants of Water in the 200-nm to 200-µm Wavelength Region, *Appl. Opt.* 12, 555-563.

Heath, D.F., A.J. Krueger, H.A. Roeder, and B.D. Henderson, The Solar Backscatter Ultraviolet and Total Ozone Mapping Spectrometer (SBUV/TOMS) for Nimbus G, *Optical Engineering*, 14, 323, 1975

Herman, J.R., and E. A. Celarier, Earth surface reflectivity climatology at 340 and 380 nm from TOMS data, J. Geophys. Res., 102, 28, 003-28, 011, 199

Hsu, N.C., J.R. Herman, P.K. Bhartia, C.J. Seftor, O.Torres, A.M. Thompson,J.F. Gleason, T.F. Eck, and B. N. Holben, Detection of biomass burning smoke from TOMS measurements, *Geophys. Res. Lett*., 23, 745-748, 1996

Hsu, N.C., J.R. Herman, J. Gleason, O. Torres and C.J. Seftor, Satellite detection of smoke aerosols over a snow/ice surface by TOMS, *Geophys. Res. Lett*., 26, 1165-1168, 1999

King, M. D., Platnick, S., Menzel, W. P., Ackerman, S. A., and Hubanks, P. A.: Spatial and Temporal Distribution of Clouds Observed by MODIS Onboard the Terra and Aqua Satellites, *IEEE T. Geosci. Remote*, 51, 3826–3852, doi:10.1109/TGRS.2012.2227333, 2013.

Levelt, P.F., E. Hilsenrath, G.W. Leppelmeier, G.H.J. van den Ooord, P.K. Bhartia, J. Taminnen, J.F. de Haan, and J.P. Veefkind, Science Objectives of the Ozone Monitoring Instrument, *IEEE Trans. Geo. Rem. Sens,*. Special Issue of the EOS-Aura mission, 44(5), 1093-1101, 2006

McPeters, et al., Nimbus-7 Total Ozone Mapping Spectrometer (TOMS) data products user's guide, NASA Reference Publication 1384, pp1-67, 1996

Torres, O., Ahn, C., and Chen, Z.: Improvements to the OMI near UV aerosol algorithm using A-train CALIOP and AIRS observations, Atmos. Meas. Tech., 6, 5621-5652, doi:10.5194/amtd-6-5621-2013, 2013

Torres, O., P.K. Bhartia, J.R. Herman and Z. Ahmad, Derivation of aerosol properties from satellite measurements of backscattered ultraviolet radiation. Theoretical Basis, J. Geophys. Res., 103, 17099-17110, 1998

Torres, O., and L. Remer, 2013, History of passive remote sensing of aerosol from space, ch.7 in *Aerosol Remote Sensing*, J. Lenoble, L. Remer, and D. Tanre, editors, Springer-Praxis, ISBN 978-3-642-17724-8, doi:10.1007/978-3-642-17725-5

Torres, O., A. Tanskanen, B. Veihelman, C. Ahn, R. Braak, P.K. Bhartia, P. Veefkind, and P. Levelt (2007), Aerosols and Surface UV Products from OMI Observations: An Overview , J. Geophys. Res., 112, D24S47, doi:10.1029/2007JD008809

Torres, O., H. Jethva, and P.K. Bhartia, Retrieval of Aerosol Optical Depth above Clouds from OMI Observations: Sensitivity Analysis and Case Studies, Journal. Atm. Sci., 69, 1037-1053, doi:10.1175/JAS-D-11-0130.1, 2012

Torres, O., et al., (2017), Impact of the Ozone Monitoring Instrument Row Anomaly on the Long-term Record of Aerosol Products, *in preparation*